

Axi-Higgs portal Dark Matter via Wess-Zumino mechanism

Akshay Anilkumar, Mathew Thomas Arun, and Arjun S. Nair

School of Physics, Indian Institute of Science Education and Research, Thiruvananthapuram-695551, Kerala, India

Abstract

We study the axion portal between the visible and the dark sector, where the Dark Matter is charged under a simple abelian extension of the Standard Model. In general, such models are anomalous and are rendered gauge invariant by a Stückelberg axion through Wess-Zumino/Green-Schwarz mechanism. This axion mixes with other Goldstone bosons in the model to give a physical axi-Higgs which becomes massive upon breaking the anomalous gauge group. Such axi-Higgs fields charged under the anomalous symmetry act as mediators for the Dark Matter annihilation to Standard Model particles and can lead to an efficient freeze-out mechanism. Here, we show that the Stückelberg axion and the resultant axi-Higgs, with its appropriate shift symmetry cancels the quantum anomalies and also generate the observed relic density for the Dark Matter. Moreover, we show that the relevant parameter space in our model, where photon production dominates, is safe from *Fermi*LAT, Cherenkov Telescope Array, and H.E.S.S. indirect detection experiments.

1 Introduction

The origin of Dark Matter is probably one of the most relevant discussions in High Energy Physics and cosmology, currently. Though it is overwhelmingly present in astrophysical and cosmological contexts [1, 2, 3, 4], its lack of evidence in terrestrial experiments poses a conundrum. This, along with the absence of a natural Dark Matter candidate in the Standard Model put forth compelling reasons for going beyond the current understanding of particle physics. One of the most successful paradigms in DM modeling is the thermal freeze-out scenario [5, 6, 7, 8, 9, 10, 11, 12, 13, 14]. Here the Dark Matter density decouples from thermal equilibrium with visible sector when its annihilation rate becomes of the order of Hubble expansion rate, at some temperature during the evolution of our universe. The annihilation of the DM particle to the Standard Model are facilitated via an interaction between the dark and visible sectors by modifying either the gauge group or the space-time symmetries in Standard Model. For such Dark Matter candidates, constraints from various direct and indirect detection experiments and their production at the *Large Hadron Collider* (LHC) become relevant. Most such extensions of SM with spontaneous breaking of the symmetry contain light pseudo-Goldstone bosons like axions or axion-like particles (ALPs) which could be searched for at colliders and can themselves mediate an efficient portal between these dark and visible sectors [15, 16, 17, 18, 19, 20].

Appending the gauge sector of Standard Model with abelian or non-abelian gauge groups are well motivated in string theory with intersecting D-branes [21, 22, 23, 24, 25, 26, 27], but they are plagued with gauge anomalies. While in beyond Standard Model field theoretic scenarios, discussed widely in literature, the most common method to cancel such tri-linear gauge anomalies is through suitably distributing the charges among fermions of each generation. Several proposals from string theory [21] and extra dimensions have brought in new perspectives regarding the cancellation of these anomalies with higher dimensional operators. These proposals include the introduction of a Wess-Zumino and a Chern-Simons term in the Lagrangian, leading to a local Wess-Zumino (WZ) mechanism [28, 29, 30] in field theory and non-local Green-Schwarz (GS) mechanism [31, 32, 33] in string theory. In such cases, the reducible anomalies vanish through the introduction of new counterterms. Though WZ and GS mechanisms are closely related [34, 35], in the former the anomaly cancellation occurs at the Lagrangian level by the shift symmetry of a Stückelberg axion that couples to the Wess-Zumino term, while the latter mechanism cancels the longitudinal components of the anomalous vertex, thus restoring the gauge invariance. Since in the GS mechanism, the Stückelberg axion is integrated out to generate non-local forms, for the purpose of this work, we consider the Wess-Zumino mechanism for anomaly cancellations and generation of interactions.

In this article, we append the Standard Model gauge group with a local anomalous $U(1)'$ and assume that the fermions are charged under them. In such models, understanding the importance of the Wess-Zumino mechanism is necessary at the level of model building. Since irreducible anomalies are absent in this anomalous $U(1)'$ extension, the gauge invariance can be restored by the WZ anomaly cancellation mechanism by including a Stückelberg axion that couples to 4-forms $F_I \wedge F_J$ of the gauge fields (I, J) . We also extend the Standard Model matter sector to include a fermionic dark matter candidate and a complex scalar, both charged under the $U(1)'$. Though it might seem that the Stückelberg axion in the WZ mechanism is eaten away by the new Z' boson, in the presence of a complex scalar field, the Stückelberg axion mixes with the complex scalar field to produce a physical pseudo-Goldstone field [36].

We will, here, show that these physical, pseudo-Goldstone bosons (namely axi-Higgs), mediate an efficient portal between the dark and the visible sectors to generate the observed dark matter relic density in the universe. In fact, the most dominant channels include $DM + DM \rightarrow W^+W^-, \gamma Z, \gamma\gamma$ and ZZ , for heavier Dark Matter masses, generated by the Wess-Zumino term.

To explain the working of the framework, we consider two models, anomalous $U(1)'_{L_\mu-L_\tau}$ and anomalous $U(1)'_{L_e+L_\mu+L_\tau}$. Here, we do not include the interactions of quarks for simplicity. In these scenarios, we show that the relic density constraint is not only satisfied, but the interesting parameter space is well within the indirect detection results of *Fermi*LAT [37, 38], Cherenkov Telescope Array [39, 40] and H.E.S.S. [41].

This article is organised as follows. In Sec.2 we briefly recapitulate the Wess-Zumino mechanism for gauge anomaly cancellation and the mixing of Stückelberg axion with the Goldstone boson. In Sec.3 we describe a generic anomalous $U(1)'$ extension to the Standard Model, along with a complex scalar field and a fermionic dark matter. We then consider two concrete models, the anomalous $U(1)'_{L_\mu-L_\tau}$ and the anomalous $U(1)'_{L_e+L_\mu+L_\tau}$ where we derive the axi-Higgs couplings with gauge bosons and fermions. In Sec.4 we compute the relic density of dark matter in these models and in Sec.5 we constraint our model with data from *Fermi*LAT, Cherenkov Telescope Array and H.E.S.S.. Finally, we summarise our results in Sec.6.

2 Wess-Zumino anomaly cancellation mechanism and axi-Higgs

In this section, we will briefly discuss the Wess-Zumino anomaly cancellation mechanism [28].

To discuss the mechanism, let's consider a single fermion field that transforms under two abelian gauge fields. This Lagrangian could be written as,

$$\begin{aligned} \mathcal{L} = & -\frac{1}{4}F_{\mu\nu}F^{\mu\nu} - \frac{1}{4}Z'_{\mu\nu}Z'^{\mu\nu} + \bar{\psi}i\gamma^\mu(\partial_\mu + ieA_\mu + ig\gamma^5 Z'_\mu)\psi \\ & + \frac{ge^2 C^{BAA}}{48\pi^2 f_b}(a+b)F_{\mu\nu}\tilde{F}^{\mu\nu} + \frac{g^3 C^{BBB}}{48\pi^2 f_b}(a+b)Z'_{\mu\nu}\tilde{Z}'^{\mu\nu} \\ & + \frac{1}{2}(\partial_\mu b + f_b Z'_\mu)^2 - \frac{1}{2}(\partial_\mu a + f_b Z'_\mu)^2, \end{aligned} \quad (1)$$

where we have introduced a Stückelberg term for the Z'_μ gauge boson with axions a and b , but the axion a is considered to be ghost-like. Note that the A_μ remains massless in the model to all orders, whereas the anomalous corrections to the one-loop effective action arise from the BBB and BAA trilinear gauge vertex. The one-loop anomalous vertices and counterterms in the WZ case are shown in Fig.1. In the GS mechanism, integrating out the axion fields generates the required non-local terms,

$$C^{BAA}\langle\partial Z'(x)\square^{-1}(x-y)F_{\mu\nu}\tilde{F}^{\mu\nu}\rangle + C^{BBB}\langle\partial Z'(x)\square^{-1}(x-y)Z'_{\mu\nu}\tilde{Z}'^{\mu\nu}\rangle, \quad (2)$$

while imposing the transversality condition $\partial_\mu Z'^\mu = 0$ on the Lagrangian. By this, the Green-Schwarz vertices (generated via the $b\partial_\mu Z'_\mu$ mixing) subtract out the longitudinal components of the anomaly, making the model gauge-invariant to all orders.

In the Wess-Zumino mechanism, the ghost term is removed and R_ξ gauge is introduced in Eq.1. Here, the mixing

terms like $b\partial_\mu Z'^\mu$ vanish from the Lagrangian. Thus, the Lagrangian in the WZ scheme is given by,

$$\begin{aligned}\mathcal{L} = & -\frac{1}{4}F_{\mu\nu}F^{\mu\nu} - \frac{1}{4}Z'_{\mu\nu}Z'^{\mu\nu} + \bar{\psi}i\gamma^\mu(\partial_\mu + ieA_\mu + ig\gamma^5 Z'_\mu)\psi \\ & + \frac{g^3 C^{BAA}}{48\pi^2 f_b} b F_{\mu\nu}\tilde{F}^{\mu\nu} + \frac{g^3 C^{BBB}}{48\pi^2 f_b} b Z'_{\mu\nu}\tilde{Z}'^{\mu\nu} \\ & + \frac{1}{2}(\partial_\mu b + f_b Z'_\mu)^2 + L_{R_\xi} .\end{aligned}\quad (3)$$

Unlike the GS mechanism, here the local description of the Lagrangian allows real trilinear Wess-Zumino interaction term of the axion, even in the broken phase. Before we describe our model, we should address the fact that the



Figure 1: Feynman diagrams showing the anomalies and counterterms. The first figure is the anomalous contribution and the second is the Chern-Simons interaction. The third and fourth figures are the Wess-Zumino term and the ALP-gauge boson mixing contribution to the Green-Schwarz mechanism.

Stükelberg axion described previously is not a real degree of freedom. This axion, in the Stükelberg term, is eaten away to become the longitudinal component of the new gauge boson. On the other hand, in the presence of other scalars in the model, the Stükelberg axion mixes with them, and integrating out the axion becomes non-trivial. Here we consider the Standard Model matter content appended by a fermionic Dark Matter (χ) and a scalar field (ϕ). The scalar part of the Lagrangian contains the new scalar field and the Stükelberg field, and is given by,

$$\mathcal{L}_{scalar} = (D_\mu \phi)^\dagger (D^\mu \phi) - m_\phi^2 \phi^\dagger \phi + \frac{1}{2}(\partial_\mu b + f_b Z'_\mu)^2 , \quad (4)$$

where $D_\mu = \partial_\mu - e_\phi g_{Z'} Z'_\mu$. Assuming that the new scalar field has a non-zero *vacuum expectation value*,

$$\phi = \frac{1}{\sqrt{2}}(v + \phi_1)e^{i\frac{\phi_2}{v}} , \quad (5)$$

the above Lagrangian, up to bilinear in fields, becomes,

$$\begin{aligned}\mathcal{L}_{scalar} = & \frac{1}{2}(\partial_\mu \phi_1)^2 - \frac{1}{2}m_\phi^2 \phi_1^2 \\ & + \frac{1}{2}(\partial_\mu \phi_2)^2 + \frac{1}{2}(\partial_\mu b)^2 + \frac{1}{2}(f_b^2 + (e_\phi g_{Z'} v)^2)Z'_\mu Z'^\mu + Z'_\mu \partial^\mu (f_b b + e_\phi g_{Z'} v \phi_2) .\end{aligned}\quad (6)$$

The first line in the above Lagrangian is the real scalar field, and the second line contains the mixing of the Goldstone boson with the axion in the model. Upon diagonalising these terms we get,

$$\begin{aligned}\mathcal{L}_{scalar} = & \frac{1}{2}(\partial_\mu \phi_1)^2 - \frac{1}{2}m_\phi^2 \phi_1^2 \\ & + \frac{1}{2}(\partial_\mu G_1)^2 + \frac{1}{2}(\partial_\mu G_2)^2 + \frac{1}{2}m_{Z'}^2 Z'_\mu Z'^\mu + m_{Z'} Z'_\mu \partial^\mu G_2 ,\end{aligned}\quad (7)$$

where $m_{Z'}^2 = (f_b^2 + (e_\phi g_{Z'} v)^2)$. The Goldstone boson fields G_1 and G_2 in the rotated basis are given as,

$$\begin{aligned}G_1 &= \frac{1}{m_{Z'}}(-f_b \phi_2 + e_\phi g_{Z'} v b) , \\ G_2 &= \frac{1}{m_{Z'}}(e_\phi g_{Z'} v \phi_2 + f_b b) .\end{aligned}\quad (8)$$

In this basis, note that G_1 , namely the axi-Higgs, is massless, and the mixing term between Z'_μ and G_2 gets cancelled on using the generalised R_ξ gauge,

$$\mathcal{L}_{R_\xi} = \frac{1}{\sqrt{\xi}}(\partial_\mu Z'^\mu - \xi m_{Z'} G_2). \quad (9)$$

Moreover, the mass of the Goldstone boson G_2 is gauge dependent and it becomes non-dynamical in the unitary gauge. Hence we are left with only one physical Goldstone boson G_1 .

Upon including the $U(1)'$ breaking terms in the scalar Lagrangian, [36],

$$V_{\mathcal{U}} = b_1(\phi e^{-ie_\phi g_{Z'} \frac{b}{f_b}}) + \lambda_1(\phi e^{-ie_\phi g_{Z'} \frac{b}{f_b}})^2 + 2\lambda_2(\phi^* \phi)(\phi e^{-ie_\phi g_{Z'} \frac{b}{f_b}}) + c.c. \quad (10)$$

this Goldstone field becomes massive. The mass of the pseudo-Goldstone boson G_1 now becomes,

$$m_{G_1}^2 = -\frac{1}{2}c_{G_1}v^2(1 + (e_\phi g_{Z'}v)^2/f_b^2) = -\frac{1}{2}c_{G_1}v^2\frac{m_{Z'}^2}{f_b^2}, \quad (11)$$

where $c_{G_1} = 4(\frac{b_1}{v^3} + 4\frac{\lambda_1}{v^2} + 2\frac{\lambda_2}{v})$. Now, the field in the un-rotated and the rotated basis are related as,

$$\begin{aligned} \phi_2 &= \frac{1}{m_{Z'}}(-f_b G_1 + e_\phi g_{Z'} v G_2), \\ b &= \frac{1}{m_{Z'}}(e_\phi g_{Z'} v G_1 + f_b G_2). \end{aligned} \quad (12)$$

Below, we will discuss how the anomalous interaction terms in Eq.3 will contribute to additional annihilation channels for fermionic Dark Matter.

3 Anomalous $U(1)'$ extension of the Standard Model

One of the first possible imminent discoveries at the *Large Hadron Collider* (LHC) would be a neutral gauge boson with a mass of $\mathcal{O}(\text{TeV})$. Various minimal extensions to the SM consider an enlarged gauge structure with abelian groups. These models predict resonances that could be searched at colliders, and the field has received attention due to the prediction of many such anomalous abelian gauge groups in D-brane models. On the other hand, such minimal extensions bring in gauge anomalies, which are either cancelled by a careful choice of gauge quantum numbers or a Stückelberg axion, as described in the previous section. Here we are interested in studying an anomalous $U(1)'$ extension to the Standard Model in a non-renormalisable effective field theory and the axi-Higgs present in the model.

| Field | $SU(3)_C$ | $SU(2)_W$ | $U(1)_Y$ | $U(1)'$ |
|----------|-----------|-----------|----------|---|
| Q_L^i | 3 | 2 | 1/3 | $e_{q_L}^i = (e_{q_L}^1, e_{q_L}^2, e_{q_L}^3)$ |
| u_R^i | 3 | 1 | 4/3 | $e_{u_R}^i = (e_{u_R}, e_{c_R}, e_{t_R})$ |
| d_R^i | 3 | 1 | -2/3 | $e_{d_R}^i = (e_{d_R}, e_{s_R}, e_{b_R})$ |
| L_L^i | 1 | 2 | -1 | $e_{\ell_L}^i = (e_{\ell_L}^1, e_{\ell_L}^2, e_{\ell_L}^3)$ |
| e_R^i | 1 | 1 | -2 | $e_{\ell_R}^i = (e_{e_R}, e_{\mu_R}, e_{\tau_R})$ |
| χ_L | 1 | 1 | 0 | e_{χ_L} |
| χ_R | 1 | 1 | 0 | e_{χ_R} |
| ϕ | 1 | 1 | 0 | e_ϕ |
| H | 1 | 2 | 1 | 0 |

Table 1: Particle content of the $U(1)'$ model. The Weyl fermions χ_L and χ_R are the left-handed and right-handed Dark Matter particles and ϕ is the new scalar field that spontaneously breaks the $U(1)'$ symmetry. $i = 1, 2, 3$ denotes the generation index.

To accommodate the massive vector boson, let's consider the extended Standard Model gauge group $SU(3)_C \times SU(2)_W \times$

$U(1)_Y \times U(1)'$, and matter content as given in Tab.1. The new abelian field being anomalous, leads to triangle diagrams with coefficients,

$$\begin{aligned}
U(1)' - U(1)' - U(1)' & : \mathcal{A}^{(0)} = \sum_f Q_f^3 , \\
U(1)' - U(1)' - U(1)_Y & : \mathcal{A}^{(1)} = \sum_f Q_f^2 Y_f , \\
U(1)' - U(1)_Y - U(1)_Y & : \mathcal{A}^{(2)} = \sum_f Q_f Y_f^2 , \\
U(1)' - SU(2)_W - SU(2)_W & : \mathcal{A}^{(3)} = \sum_f Q_f Tr[T_k T_k] , \\
U(1)' - SU(3)_c - SU(3)_c & : \mathcal{A}^{(4)} = \sum_f Q_f Tr[\tau_k \tau_k] ,
\end{aligned} \tag{13}$$

where f runs over all the fermions in Tab.1, (Y_f, Q_f) are the corresponding charges of $(U(1)_Y, U(1)')$ abelian gauge groups and (T_k, τ_k) are the generators of $(SU(2)_W, SU(3)_c)$ respectively such that they satisfy $Tr[T_i T_j] = \frac{1}{2} \delta_{ij} = Tr[\tau_i \tau_j]$ and $Tr[T_i] = 0 = Tr[\tau_i]$. To cancel these anomalous contributions, we introduce the Stückelberg axion interaction,

$$\mathcal{L}_b = \frac{1}{48\pi^2} \frac{g_{Z'}}{f_b} b(x) \left(C_1 g_{Z'}^2 Z'_{\mu\nu} \tilde{Z}'^{\mu\nu} + C_2 g_Y g_{Z'} Y_{\mu\nu} \tilde{Z}'^{\mu\nu} + C_3 g_Y^2 Y_{\mu\nu} \tilde{Y}^{\mu\nu} + C_4 g_W^2 W_{\mu\nu} \tilde{W}^{\mu\nu} + C_5 g_G^2 G_{\mu\nu} \tilde{G}^{\mu\nu} \right) , \tag{14}$$

Using the matter content in Tab.1, we then get,

$$\begin{aligned}
C_1 &= 6e_q^3 - 3e_u^3 - 3e_d^3 + 6e_l^3 - 3e_e^3 + e_{\chi_L}^3 - e_{\chi_R}^3 , \\
C_2 &= 2e_q^2 - 4e_u^2 + 2e_d^2 - 6e_l^2 + 6e_e^2 , \\
C_3 &= 2/3e_q - 16/3e_u - 4/3e_d + 6e_l - 12e_e , \\
C_4 &= 6e_q + 6e_l , \\
C_5 &= 18e_q - 9e_u - 9e_d .
\end{aligned} \tag{15}$$

After the Electro-weak symmetry breaking, $SU(2)_W \times U(1)_Y \rightarrow U(1)_{em}$, the W_μ and Y_μ bosons mix to give rise to massive Z_μ and the massless photon γ . The resultant interaction Lagrangian of the axion becomes,

$$\begin{aligned}
\mathcal{L}_b &= \frac{1}{12} g_{Z'} b(x) \left(g_{b\gamma\gamma} F_{\mu\nu} \tilde{F}^{\mu\nu} + g_{bZ\gamma} F_{\mu\nu} \tilde{Z}^{\mu\nu} + g_{bZZ} Z_{\mu\nu} \tilde{Z}^{\mu\nu} + g_{bWW} W_{\mu\nu}^+ \tilde{W}^{-\mu\nu} \right. \\
&\quad \left. + g_{bZ'Z'} Z'_{\mu\nu} \tilde{Z}'^{\mu\nu} + g_{b\gamma Z'} F_{\mu\nu} \tilde{Z}'^{\mu\nu} + g_{bZZ'} Z_{\mu\nu} \tilde{Z}'^{\mu\nu} + \frac{1}{4\pi^2 f_b} C_5 g_G^2 G_{\mu\nu} \tilde{G}^{\mu\nu} \right) ,
\end{aligned} \tag{16}$$

where the couplings, in the broken phase is given by,

$$\begin{aligned}
g_{b\gamma\gamma} &= \frac{C_3 g_Y^2 c_w^2 + C_4 g_W^2 s_w^2}{4\pi^2 f_b} , & g_{bZ\gamma} &= \frac{C_4 g_W^2 s_w c_w - C_3 g_Y^2 s_w c_w}{2\pi^2 f_b} , \\
g_{bZZ} &= \frac{C_3 g_Y^2 s_w^2 + C_4 g_W^2 c_w^2}{4\pi^2 f_b} , & g_{bWW} &= \frac{C_4 g_W^2}{2\pi^2 f_b} , \\
g_{bZ'Z'} &= \frac{C_1 g_{Z'}^2}{4\pi^2 f_b} , & g_{b\gamma Z'} &= \frac{C_2 g_Y g_{Z'} c_w}{4\pi^2 f_b} , \\
g_{bZZ'} &= \frac{-C_2 g_Y g_{Z'} s_w}{4\pi^2 f_b} .
\end{aligned} \tag{17}$$

In the above equation, $g_{Z'} = \sqrt{\frac{m_{Z'}^2 - f_b^2}{e_\phi^2 v^2}}$ and s_w and c_w are the sine and cosine of the Weinberg angle respectively.

With the extended Standard Model, the Lagrangian density of the matter content becomes,

$$\begin{aligned}
\mathcal{L}_{fermion} &= \sum_{i=1}^3 \left(\bar{Q}_L^i i \not{D} Q_L^i + \bar{u}_R^i i \not{D} u_R^i + \bar{d}_R^i i \not{D} d_R^i + \bar{L}_L^i i \not{D} L_L^i + \bar{e}_R^i i \not{D} e_R^i \right) \\
&\quad + \bar{\chi}_L i \not{D} \chi_L + \bar{\chi}_R i \not{D} \chi_R + \mathcal{L}_{Yukawa} ,
\end{aligned} \tag{18}$$

where $\mathcal{D} = \gamma^\mu D_\mu$, with D_μ representing the covariant derivatives containing the respective gauge interactions. The Yukawa term incorporates the scalar-fermion bilinear interactions given by,

$$\mathcal{L}_{Yukawa} = -\lambda_u^{ij} \left(\frac{\phi^\dagger}{\Lambda}\right)^{r_{uij}} \bar{Q}_L^i \tilde{H} u_R^j - \lambda_d^{ij} \left(\frac{\phi^\dagger}{\Lambda}\right)^{r_{dij}} \bar{Q}_L^i H d_R^j - \lambda_\ell^{ij} \left(\frac{\phi^\dagger}{\Lambda}\right)^{n_{ij}} \bar{L}_L^i H e_R^j - \lambda_\chi \phi^\dagger \left(\frac{\phi^\dagger}{\Lambda}\right)^{n_4} \bar{\chi}_L \chi_R + \text{h.c.}, \quad (19)$$

where, $\tilde{H} = i\sigma_2 H$ and $r_{uij} = e_{q_L}^i - e_{u_R}^j$, $r_{dij} = e_{q_L}^i - e_{d_R}^j$, $n_{ij} = e_{\ell_L}^i - e_{\ell_R}^j$ and $n_4 = e_{\chi_L} - e_{\chi_R} + e_\phi$.

Upon expanding about the *vacuum expectation value* of ϕ as given in Eq.5, the Goldstone boson ϕ_2 appears as phase and can be rotated away from the Yukawa terms by redefining the fermions. Instead, they re-emerge as interaction terms from the kinetic term of the fermions. Working in the basis in which the Electro-weak symmetry is broken, the ϕ_2 -fermion interaction becomes,

$$\mathcal{L}_{Goldstone-fermion} = \frac{r_{uii}}{2v} (m_{u^i})(\phi_2 \bar{u}^i \gamma^5 u^i) + \frac{r_{dii}}{2v} (m_{d^i})(\phi_2 \bar{d}^i \gamma^5 d^i) + \frac{n_{ii}}{2v} (m_{e^i})(\phi_2 \bar{e}^i \gamma^5 e^i) + \frac{n_4 + 1}{2v} (m_\chi)(\phi_2 \bar{\chi} \gamma^5 \chi). \quad (20)$$

where u^i , d^i , e^i and χ^i are Dirac fermions consisting of both left and right spinors.

Since the scalar field, ϕ , transforms non-trivially under $U(1)'$, its Goldstone mode mix with the Stückelberg axion as shown in the previous section. The SM Higgs field, on the other hand, do not mix with these axions since they are not charged under $U(1)'$. With this mixing, the physical Goldstone boson becomes a mixture of the axion (b) and the Goldstone (ϕ_2) as given in Eq.8 with mass given in Eq.11. The interaction of the physical pseudo-Goldstone boson (axi-Higgs), G_1 , could be found by re-writing Eq.14 and Eq.20 using Eq.8. In the gauge $\xi \rightarrow \infty$, the G_2 becomes non-dynamical and using Eq.12 we get,

$$\begin{aligned} \mathcal{L}_{G_1 BB} = & \frac{1}{12} g_{Z'} \frac{e_\phi g_{Z'v}}{m_{Z'}} G_1 \left(g_{b\gamma\gamma} F_{\mu\nu} \tilde{F}^{\mu\nu} + g_{bZ\gamma} F_{\mu\nu} \tilde{Z}^{\mu\nu} + g_{bZZ} Z_{\mu\nu} \tilde{Z}^{\mu\nu} + g_{bWW} W_{\mu\nu}^+ \tilde{W}^{-\mu\nu} \right. \\ & \left. + g_{bZ'Z} Z'_{\mu\nu} \tilde{Z}'^{\mu\nu} + g_{b\gamma Z'} F_{\mu\nu} \tilde{Z}'^{\mu\nu} + g_{bZZ'} Z_{\mu\nu} \tilde{Z}'^{\mu\nu} + \frac{1}{4\pi^2 f_b} C_5 g_G^2 G_{\mu\nu} \tilde{G}^{\mu\nu} \right), \end{aligned} \quad (21)$$

and

$$\begin{aligned} \mathcal{L}_{G_1 fermion} = & -\frac{r_{uii}}{2v} \frac{f_b m_{u^i}}{m_{Z'}} (G_1 \bar{u}^i \gamma^5 u^i) - \frac{r_{dii}}{2v} \frac{f_b m_{d^i}}{m_{Z'}} (G_1 \bar{d}^i \gamma^5 d^i) \\ & - \frac{n_{ii}}{2v} \frac{f_b m_{e^i}}{m_{Z'}} (G_1 \bar{e}^i \gamma^5 e^i) - \frac{n_4 + 1}{2v} \frac{f_b m_\chi}{m_{Z'}} (G_1 \bar{\chi} \gamma^5 \chi). \end{aligned} \quad (22)$$

Note that, here we have re-named the Lagrangian densities \mathcal{L}_b and $\mathcal{L}_{Goldstone-fermion}$ as $\mathcal{L}_{G_1 BB}$ and $\mathcal{L}_{G_1 fermion}$ respectively.

The aim of this article is to show that the Wess-Zumino interaction term of axi-Higgs, in Eq.21, and axi-Higgs fermion interaction in Eq.22 together foster an efficient portal for Dark Matter annihilation as shown in Fig.2. In this model, we consider the Dirac fermion χ to be the Dark Matter candidate and, in the next section, find the parameter space in which it satisfies the observed relic density of the Universe. Though this axi-Higgs portal mechanism can be applied to any anomalous $U(1)'$ extension of the Standard Model, for clarity of reading, we choose two simpler models.

The constraints of these axi-Higgs arise from their couplings to gauge bosons and fermions given in Eq.21 and Eq.22 respectively. Since the emphasis in the work is on axi-Higgs portal to Electro-weak gauge bosons, the axi-Higgs we consider are heavy $> \mathcal{O}(50\text{GeV})$. In this region, the main constraint arises from LHC through $g_{b\gamma\gamma}$ vertex. Note that the rest of the interaction terms given in Eq.16 are not independent, but related to each other through Eq.17. The LHC bound on $g_{b\gamma\gamma}$ arises from the process $\sigma(pp \rightarrow G_1) \times BR(G_1 \rightarrow \gamma\gamma)$, and they limit the $g_{b\gamma\gamma}$ coupling to $< 10^{-4} \text{GeV}^{-1}$. This bound can be recast into the other coefficients ($g_{bWW}, g_{bZZ}, g_{b\gamma Z}$) by using gauge invariance.

Hence, for simplicity, we consider anomalous $U'_{L_\mu - L_\tau}$ and anomalous $U'_{L_e + L_\mu + L_\tau}$ models, in which axi-Higgs do not couple to quarks and gluons. Thus the parameter space constrained by LHC and gauge invariance opens up for massive axi-Higgs. Moreover, we choose a region in which the charged leptonic flavour violations also are suppressed. The study of generic anomalous $U(1)'$ with all phenomenological considerations is reserved for future communication.

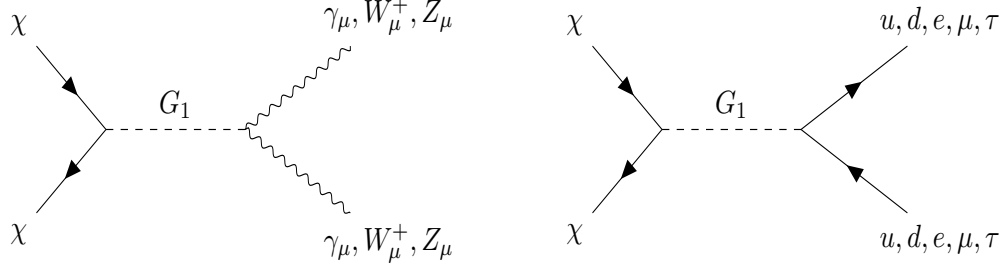


Figure 2: Diagrams that contribute to Dark Matter annihilation.

3.1 Anomalous $U'_{L_\mu-L_\tau}$

| Field | Q_L^i | u_R^i | d_R^i | L_L^i | e_R^i | χ_L | χ_R | ϕ | H |
|----------------|---------|---------|---------|-----------------------|-----------------------|----------|----------|--------|---|
| $U(1)'$ charge | 0 | 0 | 0 | $(0, e_\mu, -e_\tau)$ | $(0, e_\mu, -e_\tau)$ | 1/2 | -1/2 | -1 | 0 |

Table 2: Particle content of the anomalous $U(1)'_{L_\mu-L_\tau}$ model.

For the given set of charges for the fermions, using Eq.15, the anomaly cancellation conditions become,

$$C_1 = e_\mu^3 - e_\tau^3 + 1/4, \quad C_2 = 0, \quad C_3 = -2e_\mu + 2e_\tau, \quad C_4 = 2e_\mu - 2e_\tau, \quad C_5 = 0 \quad (23)$$

And, the Yukawa interactions in Eq.19 now becomes,

$$\mathcal{L}_{Yukawa} = -\lambda_q \bar{Q}_L \tilde{H} u_R - \lambda_d \bar{Q}_L H d_R - \lambda_e \bar{L}_L^1 H e_R^1 - \lambda_\mu \bar{L}_L^2 H e_R^2 - \lambda_\tau \bar{L}_L^3 H e_R^3 - \lambda_{mix} \left(\frac{\phi^\dagger}{\Lambda} \right)^e \bar{L}_L^2 H e_R^3 - \phi^\dagger \bar{\chi}_L \chi_R + h.c. , \quad (24)$$

where $e = e_\mu + e_\tau$.

In the above, we have the freedom to choose 'e', λ_{mix} and $\frac{\langle \phi \rangle}{\Lambda}$ such that the charged lepton mixing is suppressed, making the model free from charged lepton flavour violations. For completeness, here we take $e_\mu = 2$ and $e_\tau = 1$. In this scenario, $g_{b\gamma\gamma}$ vanishes, but though it can be generated at higher loop level, here we will not consider that. Using Eq.24 and Eq.23, the axi-Higgs couplings given in Eq.21 and Eq.22 becomes,

$$\begin{aligned} \mathcal{L}_{G_1 BB} = & -\frac{1}{12} g_{Z'} \frac{g_{Z'v}}{m_{Z'}} G_1 \left(g_{bZ\gamma} F_{\mu\nu} \tilde{Z}^{\mu\nu} + g_{bZZ} Z_{\mu\nu} \tilde{Z}^{\mu\nu} + g_{bWW} W_{\mu\nu}^+ \tilde{W}^{-\mu\nu} \right. \\ & \left. + g_{bZ'Z'} Z'_{\mu\nu} \tilde{Z}'^{\mu\nu} + g_{b\gamma Z'} F_{\mu\nu} \tilde{Z}'^{\mu\nu} + g_{bZZ'} Z_{\mu\nu} \tilde{Z}'^{\mu\nu} \right) , \end{aligned} \quad (25)$$

and

$$\mathcal{L}_{G_1 fermion} = -\frac{1}{2v} \frac{f_b m_\chi}{m_{Z'}} (G_1 \bar{\chi} \gamma^5 \chi) . \quad (26)$$

These interaction terms lead to annihilation channels for the Dark Matter $\chi\bar{\chi} \rightarrow (WW, ZZ, Z\gamma)$ as shown in the left diagram in Fig.2.

3.2 Anomalous $U(1)'_{L_e+L_\mu+L_\tau}$

The charges of the fermion and scalar fields under the $U(1)'_{L_e+L_\mu+L_\tau}$ symmetry are given in Tab.3.

| Field | Q_L^i | u_R^i | d_R^i | L_L^i | e_R^i | χ_L | χ_R | ϕ | H |
|----------------|---------|---------|---------|---------|------------|----------|----------|--------|---|
| $U(1)'$ charge | 0 | 0 | 0 | (e,e,e) | (-e,-e,-e) | 1/2 | -1/2 | -1 | 0 |

Table 3: Particle content of the anomalous $U(1)'_{L_e+L_\mu+L_\tau}$ model.

Here, the scalar field interactions are given by the Lagrangian,

$$\mathcal{L}_H = -\lambda_q \bar{Q}_L \tilde{H} u_R - \lambda_d \bar{Q}_L H d_R + \lambda_e^{ij} \left(\frac{\phi^\dagger}{\Lambda}\right)^2 \bar{L}_L^i H e_R^j + \phi^\dagger \bar{\chi}_L \chi_R. \quad (27)$$

From Eq.15, for the given set of charges for the fermions, the cancellation of the $U(1)'$ anomalies demands,

$$C_1 = 9e^3 + 1/4, \quad C_2 = 0, \quad C_3 = 18e, \quad C_4 = 6e, \quad C_5 = 0 \quad (28)$$

Like before, for simplicity, we will consider $e = 1$. Tab.3 ensures that the left-handed and right-handed leptons are charged uniformly under $U(1)'$, hence not leading to lepton flavour violating decays. For two different benchmark Z' boson masses of 2.5 TeV and 3.5 TeV, we study the different co-annihilation channels of Dark Matter to standard model particles via the axi-higgs portal, for Dark Matter mass in the range of 70 GeV to 460 GeV.

Using Eq.27 and Eq.28, the axi-Higgs couplings given in Eq.21 and Eq.22 becomes,

$$\begin{aligned} \mathcal{L}_{G_1 BB} = & -\frac{1}{12} g_{Z'} \frac{g_{Z'v}}{m_{Z'}} G_1 \left(g_{b\gamma\gamma} F_{\mu\nu} \tilde{F}^{\mu\nu} + g_{bZ\gamma} F_{\mu\nu} \tilde{Z}^{\mu\nu} + g_{bZZ} Z_{\mu\nu} \tilde{Z}^{\mu\nu} + g_{bWW} W_{\mu\nu}^+ \tilde{W}^{-\mu\nu} \right. \\ & \left. + g_{bZ'Z} Z'_{\mu\nu} \tilde{Z}'^{\mu\nu} + g_{b\gamma Z'} F_{\mu\nu} \tilde{Z}'^{\mu\nu} + g_{bZZ'} Z_{\mu\nu} \tilde{Z}'^{\mu\nu} \right), \end{aligned} \quad (29)$$

and

$$\mathcal{L}_{G_1 fermion} = -\frac{1}{v} \frac{f_b m_{e^i}}{m_{Z'}} (G_1 \bar{e}^i \gamma^5 e^i) - \frac{1}{2v} \frac{f_b m_\chi}{m_{Z'}} (G_1 \bar{\chi} \gamma^5 \chi). \quad (30)$$

These interaction terms lead to annihilation channels for the Dark Matter $\chi\bar{\chi} \rightarrow (WW, ZZ, \gamma\gamma, e^i e^i)$ as shown in Fig.2.

4 Relic Density

Since neither the particle content nor the interactions of Dark Matter is known, we do not know the origin of the observed relic density in our universe. Nevertheless, there are two popular mechanisms that explain the observed abundance of Dark Matter - the freeze-out and the freeze-in mechanisms. In the thermal freeze-out mechanism, the Dark Matter is assumed to be initially in thermal equilibrium with the rest of the cosmic plasma. As the universe cooled and the temperature dropped below ~ 0.05 times the mass of the Dark Matter, the Hubble expansion rate (the expansion rate of the Universe) exceeded the annihilation rate and they decoupled from the visible sector. As mentioned in Sec.1, in this article we consider a Weakly Interacting Massive Particle (WIMP) freeze-out Dark Matter. Hence, the DM is assumed to freeze-out when the DM annihilation rate, Γ , is of the order of the Hubble rate H [42] i.e.,

$$\Gamma = n_{eq} \langle \sigma v \rangle \sim H. \quad (31)$$

Here, n_{eq} is the Dark Matter number density when it is in thermal equilibrium with the Standard Model particles and the photon bath and $\langle \sigma v \rangle$ is the velocity-averaged annihilation cross section.

In our model, the Dark Matter number density today is calculated by the evolution of the $2 \rightarrow 2$ inelastic scattering processes shown in Fig.2 using the Boltzmann equation,

$$\frac{dn}{dt} + 3Hn = -\langle \sigma v \rangle (n^2 - n_{eq}^2), \quad (32)$$

where n is the number density of DM. This relation is guided by the thermally averaged cross-section which is defined as,[43]

$$\langle \sigma v \rangle (T) = \frac{1}{8m_\chi^4 T K_2^2(m_\chi/T)} \int_{4m_\chi^2}^{\infty} d\tilde{s} \sigma(\tilde{s}) (\tilde{s} - 4m_\chi^2) \sqrt{\tilde{s}} K_1 \frac{\sqrt{\tilde{s}}}{T} \quad (33)$$

where K_i denotes the modified Bessel function of order i and $\tilde{s} = (p_1 + p_2)^2$, p_1 and p_2 being the four momenta of the annihilating dark matter particles. The annihilation cross-sections σ are computed for each process shown in Fig.2 , and they become,

$$\begin{aligned}
\sigma(\chi\bar{\chi} \rightarrow W^+W^-) &= \left(\frac{-f_b m_\chi}{2vm_{Z'}}\right)^2 \frac{g_{bWW}^2 \tilde{s}(\tilde{s} - 4m_W^2)}{16\pi((m_{G_1}^2 - \tilde{s})^2 + m_{G_1}^2 \Gamma_{G_1}^2)} \\
\sigma(\chi\bar{\chi} \rightarrow ZZ) &= \left(\frac{-f_b m_\chi}{2vm_{Z'}}\right)^2 \frac{g_{bZZ}^2 \tilde{s}(\tilde{s} - 4m_Z^2)}{16\pi((m_{G_1}^2 - \tilde{s})^2 + m_{G_1}^2 \Gamma_{G_1}^2)} \\
\sigma(\chi\bar{\chi} \rightarrow \gamma\gamma) &= \left(\frac{-f_b m_\chi}{2vm_{Z'}}\right)^2 \frac{g_{b\gamma\gamma}^2 \tilde{s}^2}{16\pi((m_{G_1}^2 - \tilde{s})^2 + m_{G_1}^2 \Gamma_{G_1}^2)} \\
\sigma(\chi\bar{\chi} \rightarrow \gamma Z) &= \left(\frac{-f_b m_\chi}{2vm_{Z'}}\right)^2 \frac{g_{b\gamma Z}^2 (\tilde{s} + m_Z^2)^2}{16\pi((m_{G_1}^2 - \tilde{s})^2 + m_{G_1}^2 \Gamma_{G_1}^2)} \\
\sigma(\chi\bar{\chi} \rightarrow e^i \bar{e}^i) &= \left(\frac{-f_b m_\chi}{2vm_{Z'}}\right)^2 \left(\frac{-f_b m_{e^i}}{vm_{Z'}}\right)^2 \frac{\tilde{s}}{16\pi((m_{G_1}^2 - \tilde{s})^2 + m_{G_1}^2 \Gamma_{G_1}^2)} .
\end{aligned} \tag{34}$$

Rewriting Eq.32 with the abundance $Y = \frac{n}{s}$, where s is the total entropy density of the universe, the evolution of the DM abundance with the evolution of the universe, with the rescaled time variable $x = m/T$, is described by,

$$\frac{dY}{dx} = -\frac{xs \langle \sigma v \rangle}{H(m)} (Y^2 - Y_{eq}^2) . \tag{35}$$

Using the solution for DM abundance today from the above equation, for a CDM in the freeze-out scenario, the relic density is given by,

$$\Omega h^2 = \frac{m_\chi Y_\infty s_0 h^2}{\rho_c} \sim \frac{10^{-26} cm^3 s^{-1}}{\langle \sigma v \rangle} , \tag{36}$$

where Y_∞ and s_0 are the present-day DM yield and entropy density respectively, and ρ_c is the critical density. Comparing this with critical dark matter density observed by the *Planck* collaboration [44],

$$\Omega h_{critical}^2 = 0.120 \pm 0.001 , \tag{37}$$

constraints the parameter space allowed in our model.

We use **micrOMEGAs 5.3.41** [45] for calculating the relic density for different parameters for the two models we described in subsections 3.1 and 3.2. Since in either of these models, the Dark Matter do not interact with quarks or gluons, *Large Hadron Collider* and direct detection bounds are relaxed.

To compute the relic density, we consider two benchmark points for the mass of the Z' boson, $m_{Z'} = 2.5$ TeV and $m_{Z'} = 3.5$ TeV. Using the relation $m_{Z'}^2 = (f_b^2 + (e_\phi g_{Z'} v)^2)$, for a given $g_{Z'}$, e_ϕ and v , we get an upper limit on the value of the symmetry-breaking scale f_b and hence the mass of the axi-Higgs m_{G_1} .

In the $U'_{L_\mu - L_\tau}$ model, since the charge distribution prohibits DM-fermion coupling, the dark matter can annihilate only to the gauge bosons governed by the interaction Lagrangian given in Eq.25. Hence, for lower mass range ($m_{DM} \lesssim 45$ GeV) dark matter relic density becomes higher than the observed critical value.

The variation of the relic density with dark matter mass for different values of f_b is shown in Fig.3a and Fig.3b for $m_{Z'} = 2500$ GeV and $m_{Z'} = 3500$ GeV respectively, while the mass of the axi-Higgs is related to the symmetry breaking scale f_b , as given in Eq.11, where the parameter c_{G_1} is taken to be -0.001 .

The relative contribution of different annihilation channels are shown in Fig.4. From this, we see that the W^+W^- channel serves as the most dominant annihilation channel for dark matter particles. In Tab.4, we summarise the relative contribution of annihilation channels for a set of benchmark values of m_{G_1} and corresponding dark matter m_{DM} for which the computed relic density lies within $\Omega h_{critical}^2 = 0.12 \pm 0.001$.

Similar to the previous calculations, below, we compute the relic density and contributions of the annihilation channels for the $U'_{L_e + L_\mu + L_\tau}$ model. Here, the axi-Higgs's couplings to the charged leptons are not suppressed, and hence lower dark matter masses ($m_{DM} \lesssim 50$ GeV) are allowed and we get the relic density to be within the critical

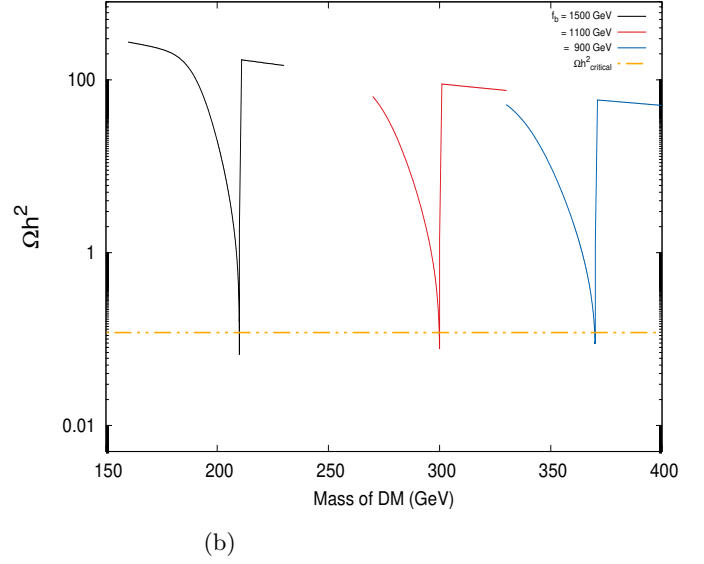
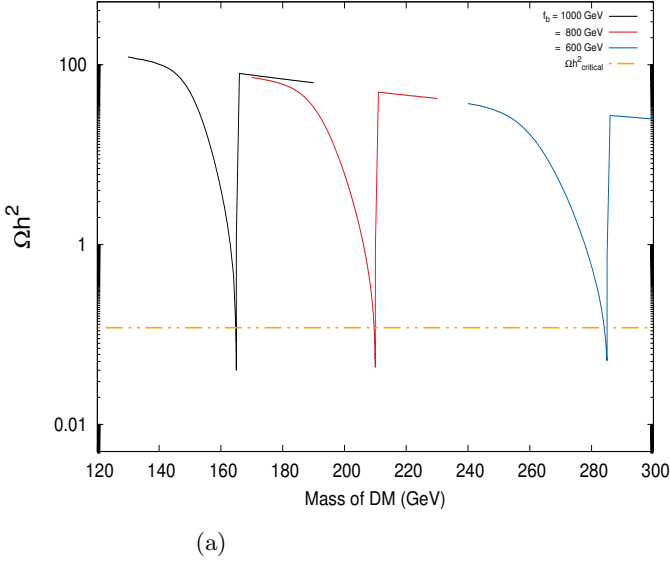


Figure 3: Plot showing the variation of relic density as a function of DM mass for different values of f_b , keeping $m_{Z'} = 2500$ GeV (left), 3500 GeV (right), $c_{G1} = -0.001$ and $g_{Z'} \sim 0.4$ for the $U'_{L\mu-L\tau}$ model. Mass of the axi-higgs is related to these parameters as $m_{G1} = \frac{m_{Z'} \sqrt{c_{G1}(m_{Z'}^2 - f_b^2)}}{\sqrt{2}g_{Z'}f_b}$.

| m_{G1} (GeV) | m_{DM} (GeV) | Annihilation channels |
|-------------------|-------------------|--|
| 330 | 164.9 | 71% $\chi\bar{\chi} \rightarrow W^+W^-$ 25% $\chi\bar{\chi} \rightarrow \gamma Z$ 4% $\chi\bar{\chi} \rightarrow ZZ$ |
| 420 | 209.6 | 72% $\chi\bar{\chi} \rightarrow W^+W^-$ 24% $\chi\bar{\chi} \rightarrow \gamma Z$ 4% $\chi\bar{\chi} \rightarrow ZZ$ |
| 570 | 284.1 | 73% $\chi\bar{\chi} \rightarrow W^+W^-$ 23% $\chi\bar{\chi} \rightarrow \gamma Z$ 4% $\chi\bar{\chi} \rightarrow ZZ$ |

| m_{G1} (GeV) | m_{DM} (GeV) | Annihilation channels |
|-------------------|-------------------|--|
| 420 | 209.9 | 72% $\chi\bar{\chi} \rightarrow W^+W^-$ 24% $\chi\bar{\chi} \rightarrow \gamma Z$ 4% $\chi\bar{\chi} \rightarrow ZZ$ |
| 600 | 299.8 | 73% $\chi\bar{\chi} \rightarrow W^+W^-$ 23% $\chi\bar{\chi} \rightarrow \gamma Z$ 4% $\chi\bar{\chi} \rightarrow ZZ$ |
| 740 | 369.7 | 73% $\chi\bar{\chi} \rightarrow W^+W^-$ 23% $\chi\bar{\chi} \rightarrow \gamma Z$ 4% $\chi\bar{\chi} \rightarrow ZZ$ |

Table 4: Benchmark points from Fig.4a and Fig.4b showing values of m_{G1} and m_{DM} for the $U(1)_{L\mu-L\tau}$ model for $m_{Z'} = 2500$ GeV (left) and 3500 GeV (right) that satisfy the observed DM relic abundance of the universe. The major annihilation channels of the dark matter and their relative contributions are shown in the third column.

value. This is shown in Fig.5a and Fig.5b for $m_{Z'} = 2500$ GeV and $m_{Z'} = 3500$ GeV respectively. And, the different annihilation channels and their relative contributions are shown in Fig.6a and Fig.6b. While the relative contribution of the bosonic channels shows a similar behaviour as the previous case for heavier dark matter, a new tau lepton channel becomes dominant at lower dark matter masses. Hence, the fermionic annihilation channel also becomes important in the $U'_{L_e+L_\mu+L_\tau}$ model. Finally, in Tab.5, we summarise the annihilation channels for a set of benchmark values of m_{G1} and corresponding m_{DM} for which the observed relic density is satisfied.

5 Indirect Detection

In the previous section, while computing the relic density, we observed that the annihilation channels for the dark matter contain a significant fraction of photon (γ) production. Such processes, with very high-energy gamma rays, are actively searched for by instruments like Fermi Gamma-ray Large Area Telescope (*Fermi*LAT) [37, 38], Cherenkov Telescope Array [39, 40] and High Energy Stereoscopic System (H.E.S.S.) [41].

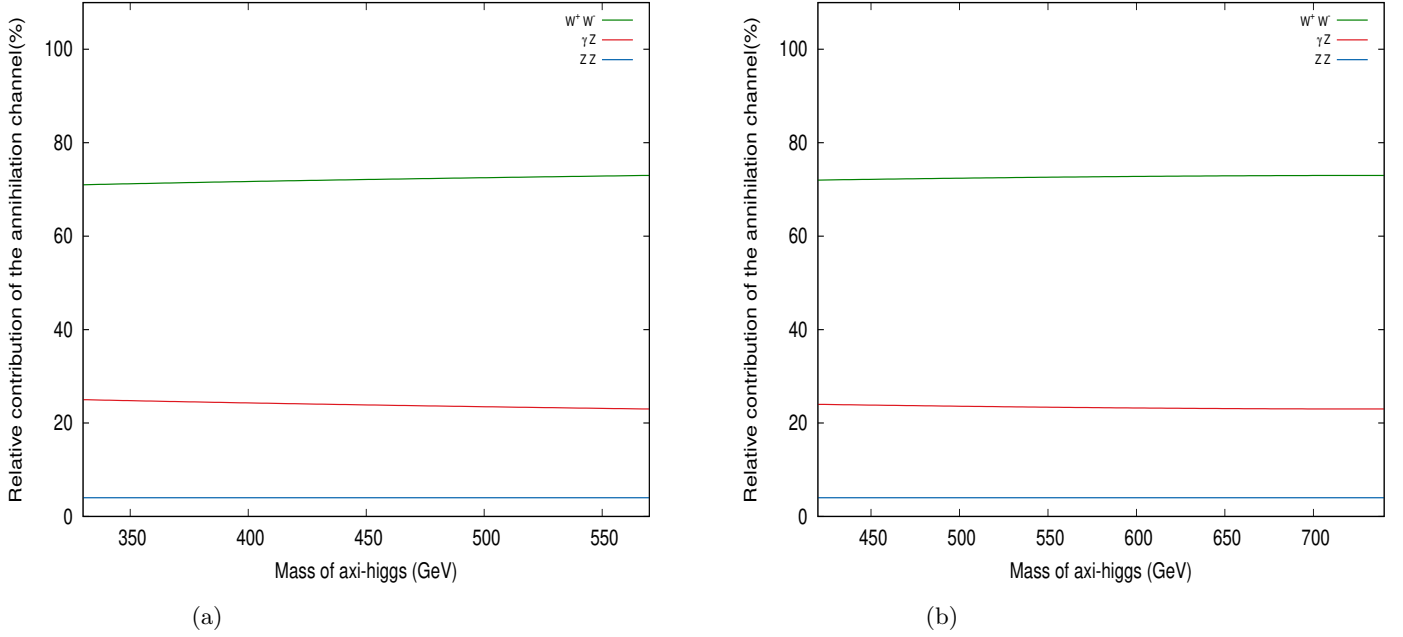


Figure 4: Relative contribution of the different annihilation channels vs mass of mediator plot for which the calculated relic density matches $\Omega h^2_{critical}$, for $m_{Z'} = 2500$ GeV (left), 3500 GeV (right), $c_{G1} = -0.001$ and $g_{Z'} \sim 0.4$ for the $U(1)'_{L_\mu-L_\tau}$ model

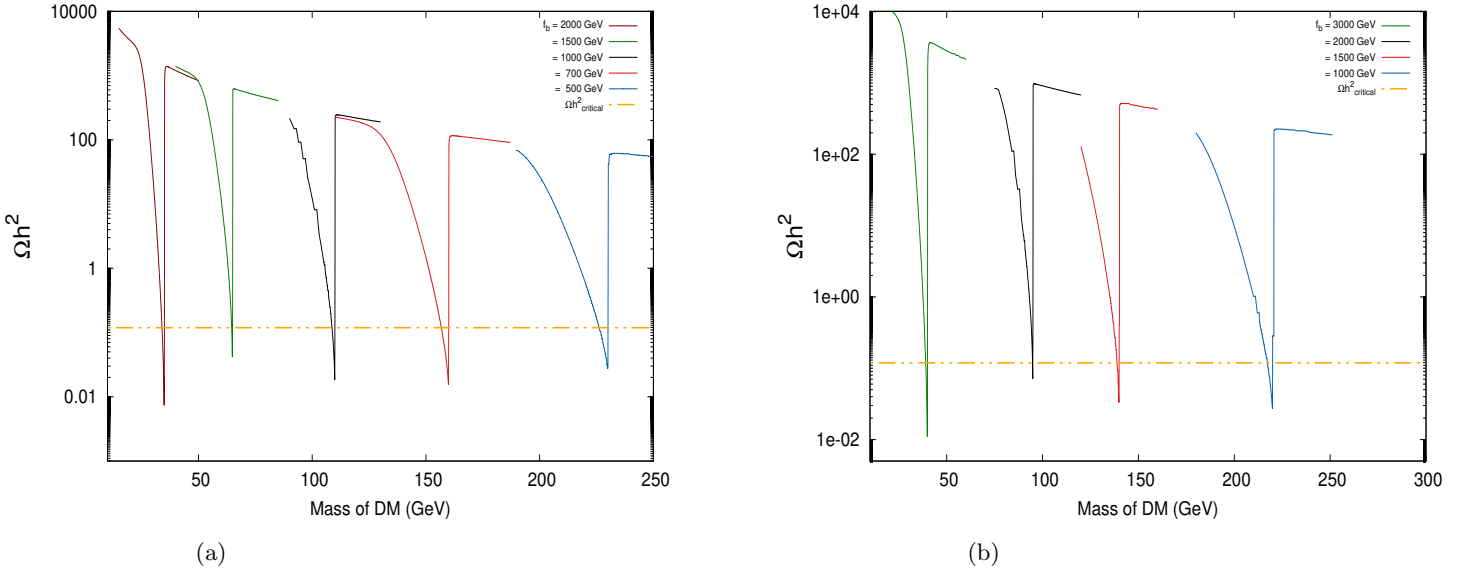


Figure 5: Plot showing the variation of relic density as a function of DM mass for different values of f_b , keeping $m_{Z'} = 2500$ GeV (left), 3500 GeV (right), $c_{G1} = -0.001$ and $g_{Z'} \sim 0.6$ for the $U'_{L_e+L_\mu+L_\tau}$ model. Mass of the axi-higgs is related to these parameters as $m_{G1} = \frac{m_{Z'} \sqrt{c_{G1}(m_{Z'}^2 - f_b^2)}}{\sqrt{2} g_{Z'} f_b}$.

While *Fermi*LAT is a satellite-based observatory that detects gamma rays in the energy range from 20 MeV to over 300 GeV, H.E.S.S. and CTA are ground-based observatories that detect very high-energy gamma-ray fluxes in the range $E_\gamma > 300\text{GeV}$ and $200\text{GeV} < E_\gamma < 300\text{TeV}$ respectively. The experiments measure the photon flux received at Earth from galactic centers, given by,

$$\frac{1}{A} \frac{dN_\gamma}{dEdt} \propto \frac{\langle \sigma v_{rel} \rangle_{X\gamma}}{m_{DM}^2} \quad (38)$$

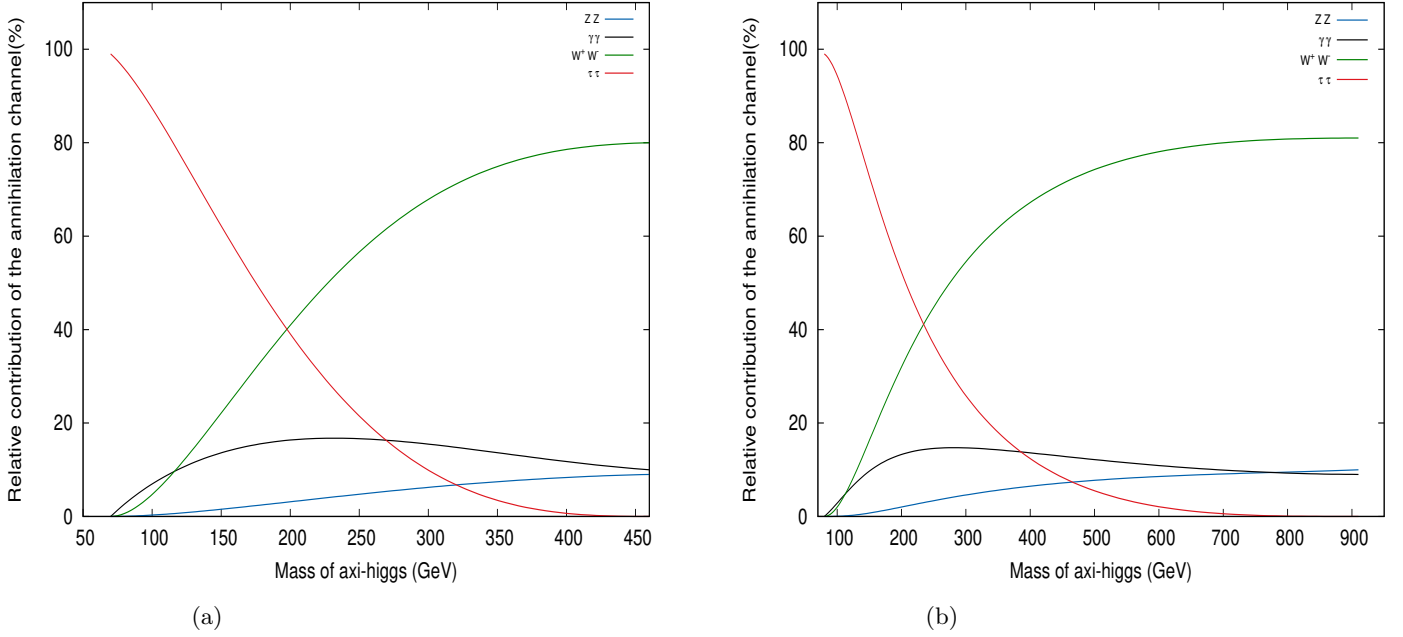


Figure 6: Relative contribution of the different annihilation channels vs mass of mediator plot for which the calculated relic density matches $\Omega h^2_{critical}$, for $m_{Z'} = 2500$ GeV (left), 3500 GeV (right), $c_{G_1} = -0.001$ and $g_{Z'} \sim 0.6$ for the $U(1)'_{L_e+L_\mu+L_\tau}$ model

| m_{G_1} (GeV) | m_{DM} (GeV) | annihilation channels |
|--------------------|-------------------|--|
| 70 | 33.9 | 99% $\chi\bar{\chi} \rightarrow \tau\tau$ |
| 130 | 64.6 | 83% $\chi\bar{\chi} \rightarrow \tau\tau$ 17% $\chi\bar{\chi} \rightarrow \gamma\gamma$ |
| 220 | 108.7 | 68% $\chi\bar{\chi} \rightarrow W^+W^-$ 23% $\chi\bar{\chi} \rightarrow \gamma\gamma$ 4% $\chi\bar{\chi} \rightarrow \tau\tau$ 4% $\chi\bar{\chi} \rightarrow ZZ$ |
| 320 | 156.7 | 79% $\chi\bar{\chi} \rightarrow W^+W^-$ 13% $\chi\bar{\chi} \rightarrow \gamma\gamma$ 8% $\chi\bar{\chi} \rightarrow ZZ$ |
| 460 | 226.0 | 80% $\chi\bar{\chi} \rightarrow W^+W^-$ 10% $\chi\bar{\chi} \rightarrow \gamma\gamma$ 9% $\chi\bar{\chi} \rightarrow ZZ$ |

| m_{G_1} (GeV) | m_{DM} (GeV) | annihilation channels |
|--------------------|-------------------|--|
| 80 | 39.1 | 99% $\chi\bar{\chi} \rightarrow \tau\tau$ |
| 190 | 94.8 | 40% $\chi\bar{\chi} \rightarrow \tau\tau$ 35% $\chi\bar{\chi} \rightarrow W^+W^-$ 24% $\chi\bar{\chi} \rightarrow \gamma\gamma$ |
| 280 | 138.8 | 76% $\chi\bar{\chi} \rightarrow W^+W^-$ 15% $\chi\bar{\chi} \rightarrow \gamma\gamma$ 7% $\chi\bar{\chi} \rightarrow ZZ$ 2% $\chi\bar{\chi} \rightarrow \tau\tau$ |
| 440 | 217.1 | 80% $\chi\bar{\chi} \rightarrow W^+W^-$ 11% $\chi\bar{\chi} \rightarrow \gamma\gamma$ 9% $\chi\bar{\chi} \rightarrow ZZ$ |

Table 5: Few benchmark points from Fig.6a and Fig.6b showing values of m_{G_1} and m_{DM} for the $U(1)'_{L_e+L_\mu+L_\tau}$ model for $M_{Z'} = 2500$ GeV (left) and 3500 GeV (right) that satisfy the observed DM relic abundance of the universe. The major annihilation channels and their relative contributions are also given.

where $\frac{dN_\gamma}{dE dt}$ denotes the energy spectrum of photons produced in the annihilation process with the velocity-averaged cross-section $\langle \sigma v_{rel} \rangle_{X\gamma}$. This velocity-averaged cross-section can be obtained from [46],

$$\langle \sigma v_{rel} \rangle_{X\gamma} = \frac{1}{m_\chi^2} \left[\omega(s)_{X\gamma} - \frac{3}{2} (2\omega(s) - 4m_\chi^2 \omega'(s)_{X\gamma}) \frac{1}{x_f} \right] \Big|_{s=4m_\chi^2} \quad (39)$$

where the function $\omega(s)$ is defined as,

$$\omega(s)_{X\gamma} = \frac{1}{32\pi} \sum_{spins} \left| \mathcal{M}_{\chi\bar{\chi} \rightarrow X\gamma} \right|^2 \quad (40)$$

where X is either γ or Z in our model.

Here, using the NFW[47] dark matter density profile, we calculate the velocity-averaged cross-section, $\langle\sigma v_{rel}\rangle$, for the production of photons from DM annihilation in both the anomalous $U(1)'$ models considered. For the $U(1)'_{L_\mu-L_\tau}$, as described in Sec.3.1, $g_{a\gamma\gamma} = 0$, and hence direct annihilation of DM into a pair of photons is not possible. However, we get photons in the final state from the $\chi\bar{\chi} \rightarrow \gamma Z$ channel and from the loop level contributions of $\chi\bar{\chi} \rightarrow W^+W^-$ and $\chi\bar{\chi} \rightarrow ZZ$. Among these, we consider only the direct channel, as the rest are higher loop suppressed. On the other hand, in the $U(1)'_{L_e+L_\mu+L_\tau}$ model, the contribution of the $\chi\bar{\chi} \rightarrow \gamma Z$ annihilation channel vanishes and a non-zero $g_{a\gamma\gamma}$ ensures that the contribution of the $\chi\bar{\chi} \rightarrow \gamma\gamma$ channel is significant.

For lower mass dark matter in the range of 10 GeV to 200 GeV, the *Fermi*LAT[38] data provides the strongest upper bounds, while for higher masses ($m_{DM} > 200$ GeV), the strongest bounds come from CTA[40]. The bounds from the H.E.S.S.[41] data are also considered. Upon comparing the $\langle\sigma v_{rel}\rangle_{X\gamma}$ calculated in our models with the experiments, we see that the parameter space that satisfies the observed relic density is allowed by these experiments. The results are shown in Fig.7 for the anomalous $U(1)'_{L_\mu-L_\tau}$ and in Fig.8 for the anomalous $U(1)'_{L_e+L_\mu+L_\tau}$ model. The grey shaded area corresponds to the region where the relic density is greater than the observed critical value, and hence ruled out. And, the region above the dashed, dash-dotted, and dotted lines are ruled out by *Fermi*LAT, CTA, and H.E.S.S. data respectively.

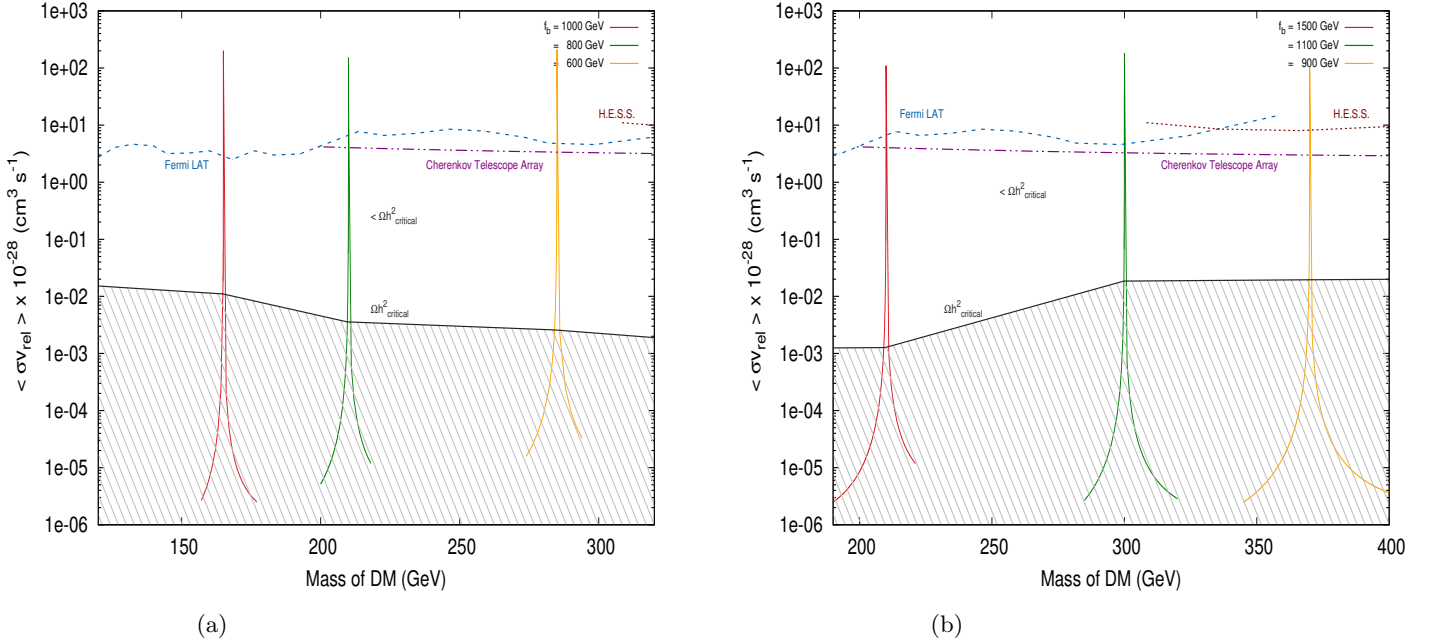


Figure 7: Velocity-averaged cross-section for $\chi\bar{\chi} \rightarrow \gamma Z$ annihilation vs mass of DM plot for the indirect detection of dark matter, for $m_{Z'} = 2500$ GeV (left), 3500 GeV (right), $c_{G_1} = -0.001$ and $g_{Z'} \sim 0.4$ for the $U'_{L_\mu-L_\tau}$ model. The grey shaded region is ruled out since the calculated relic density is more than $\Omega h^2_{critical}$ of the universe, while the region above the blue (dashed), purple (dot-dashed) and maroon (dotted) lines are excluded by indirect detection experiments - *Fermi*LAT, CTA and H.E.S.S. - respectively.

6 Conclusion

One of the simplest beyond Standard Model scenario is an extension of the Standard Model gauge group with an $U(1)'$. Such models naturally exist and are anomalous in orientifolds [21]. The gauge anomalies present in these extensions are usually cancelled, in string theory, by Green-Schwarz mechanism. In low energy effective quantum field theory framework, the Green-Schwarz term arises from the well-known Wess-Zumino interaction, $F_I \wedge F_J$, with a Stückelberg axion. This Wess-Zumino effective action provides a counterterm that cancels the anomalies rendering the model gauge invariant. Indeed, rearranging and integrating out the axions in the Wess-Zumino case generates the Green-Schwarz effective action, they are non-local and the two mechanisms are different albeit having the same origin.

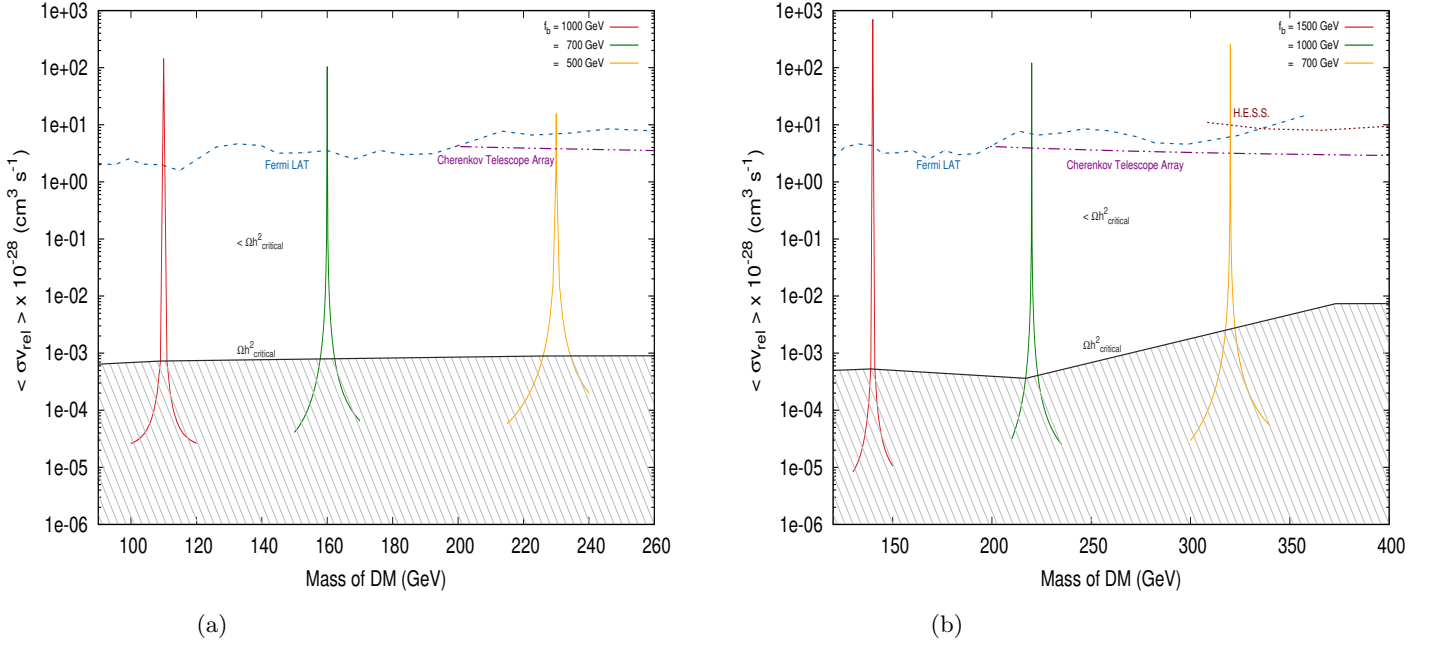


Figure 8: Velocity-averaged cross-section for $\chi\bar{\chi} \rightarrow \gamma\gamma$ annihilation vs mass of DM plot for the indirect detection of dark matter, for $m_{Z'} = 2500 \text{ GeV}$ (left), 3500 GeV (right), $c_{G1} = -0.001$ and $g_{Z'} \sim 0.6$ for the $U'_{L_e+L_\mu+L_\tau}$ model. The grey shaded region is ruled out since the calculated relic density is more than $\Omega h^2_{\text{critical}}$ of the universe, while the region above the blue (dashed), purple (dot-dashed) and maroon (dotted) lines are excluded by indirect detection experiments - *Fermi*LAT, CTA and H.E.S.S. - respectively.

The aforementioned Stückelberg axion readily mixes with other pseudo-Goldstone bosons in the theory to form axi-Higgs, which are massive and remains in the spectra after gauge fixing. Here, in this article, we are concerned with the possibility that these axi-Higgs could mediate dark matter annihilation to Standard Model fields. To this end, we consider a simple anomalous $U(1)'$ extension to the Standard Model along with a complex scalar field and fermionic Dark Matter. The complex scalar field is necessary to give the dark matter its mass. This simple extension is strikingly different from other models found in literature, owing to the fact that we do not have a multitude of fields whose charges under $U(1)'$ are carefully distributed.

For concreteness, we considered two models, an anomalous $U(1)'_{L_\mu-L_\tau}$ and anomalous $U(1)'_{L_e+L_\mu+L_\tau}$. Quarks are considered to be singlets under the abelian gauge groups, to make the work simple and clear without other constraints from hadron physics. Nevertheless, the framework can be extended to other scenarios with quark couplings as well. In these models, we compute the relic density arising from the annihilation channels $\chi\bar{\chi} \rightarrow W^+W^-, \gamma\gamma, Z\gamma, ZZ$, and $\tau\tau$. These results are shown in Fig.3 and Fig.5, and the relative contributions of these channels are computed as a function of the mediator mass and are shown Fig.4 and Fig.6. A few benchmark points are given in Tab.4 and Tab.5.

Since quarks are not charged under $U(1)'$, direct detection experiments do not constraint the models at tree-level. On the other hand, since the γ production channels exist, constraints from *Fermi*LAT, Cherenkov Telescope Array and H.E.S.S. become important and the parameter space allowed are shown in Fig.7 and Fig.8. Thus, we show here that minimal extension of Standard Model, which are anomalous, can host interesting dark matter phenomenology.

Acknowledgments

M.T.A. acknowledges the financial support of DST through the INSPIRE Faculty grant DST/INSPIRE/04/2019/002507.

References

- [1] Gianfranco Bertone, Dan Hooper, and Joseph Silk. Particle dark matter: Evidence, candidates and constraints. *Phys. Rept.*, 405:279–390, 2005.
- [2] E. Komatsu et al. Five-Year Wilkinson Microwave Anisotropy Probe (WMAP) Observations: Cosmological Interpretation. *Astrophys. J. Suppl.*, 180:330–376, 2009.
- [3] P. A. R. Ade et al. Planck 2015 results. XIII. Cosmological parameters. *Astron. Astrophys.*, 594:A13, 2016.
- [4] E. Aprile et al. Dark Matter Search Results from a One Ton-Year Exposure of XENON1T. *Phys. Rev. Lett.*, 121(11):111302, 2018.
- [5] M. I. Vysotsky, A. D. Dolgov, and Ya. B. Zeldovich. Cosmological Restriction on Neutral Lepton Masses. *JETP Lett.*, 26:188–190, 1977.
- [6] Katsuhiko Sato and Makoto Kobayashi. Cosmological Constraints on the Mass and the Number of Heavy Lepton Neutrinos. *Prog. Theor. Phys.*, 58:1775, 1977.
- [7] Benjamin W. Lee and Steven Weinberg. Cosmological Lower Bound on Heavy Neutrino Masses. *Phys. Rev. Lett.*, 39:165–168, 1977.
- [8] P. Hut. Limits on Masses and Number of Neutral Weakly Interacting Particles. *Phys. Lett. B*, 69:85, 1977.
- [9] G. Steigman. Cosmology Confronts Particle Physics. *Ann. Rev. Nucl. Part. Sci.*, 29:313–338, 1979.
- [10] Edward W. Kolb and Keith A. Olive. The Lee-Weinberg Bound Revisited. *Phys. Rev. D*, 33:1202, 1986. [Erratum: *Phys.Rev.D* 34, 2531 (1986)].
- [11] Robert J. Scherrer and Michael S. Turner. On the Relic, Cosmic Abundance of Stable Weakly Interacting Massive Particles. *Phys. Rev. D*, 33:1585, 1986. [Erratum: *Phys.Rev.D* 34, 3263 (1986)].
- [12] Kim Griest and David Seckel. Three exceptions in the calculation of relic abundances. *Phys. Rev. D*, 43:3191–3203, 1991.
- [13] Gerard Jungman, Marc Kamionkowski, and Kim Griest. Supersymmetric dark matter. *Phys. Rept.*, 267:195–373, 1996.
- [14] Giorgio Arcadi, Máira Dutra, Pradipta Ghosh, Manfred Lindner, Yann Mambrini, Mathias Pierre, Stefano Profumo, and Farinaldo S. Queiroz. The waning of the WIMP? A review of models, searches, and constraints. *Eur. Phys. J. C*, 78(3):203, 2018.
- [15] Yasunori Nomura and Jesse Thaler. Dark Matter through the Axion Portal. *Phys. Rev. D*, 79:075008, 2009.
- [16] Marat Freytsis and Zoltan Ligeti. On dark matter models with uniquely spin-dependent detection possibilities. *Phys. Rev. D*, 83:115009, 2011.
- [17] Rouven Essig et al. Working Group Report: New Light Weakly Coupled Particles. In *Snowmass 2013: Snowmass on the Mississippi*, 10 2013.
- [18] Matthew J. Dolan, Felix Kahlhoefer, Christopher McCabe, and Kai Schmidt-Hoberg. A taste of dark matter: Flavour constraints on pseudoscalar mediators. *JHEP*, 03:171, 2015. [Erratum: *JHEP* 07, 103 (2015)].
- [19] Patrick J. Fitzpatrick, Yonit Hochberg, Eric Kuflik, Rotem Ovadia, and Yotam Soreq. Dark matter through the axion-gluon portal. *Phys. Rev. D*, 108(7):075003, 2023.
- [20] Giovanni Armando, Paolo Panci, Joachim Weiss, and Robert Ziegler. Leptonic ALP portal to the dark sector. *Phys. Rev. D*, 109(5):055029, 2024.
- [21] Luis E. Ibanez, R. Rabadan, and A. M. Uranga. Anomalous $U(1)$ ’s in type I and type IIB $D = 4$, $N=1$ string vacua. *Nucl. Phys. B*, 542:112–138, 1999.

- [22] Ralph Blumenhagen, Boris Kors, Dieter Lust, and Stephan Stieberger. Four-dimensional String Compactifications with D-Branes, Orientifolds and Fluxes. *Phys. Rept.*, 445:1–193, 2007.
- [23] Ralph Blumenhagen, Mirjam Cvetič, Paul Langacker, and Gary Shiu. Toward realistic intersecting D-brane models. *Ann. Rev. Nucl. Part. Sci.*, 55:71–139, 2005.
- [24] Ignatios Antoniadis, Savas Dimopoulos, and Amit Giveon. Little string theory at a TeV. *JHEP*, 05:055, 2001.
- [25] Luis A. Anchordoqui, Ignatios Antoniadis, Karim Benakli, and Dieter Lust. Anomalous U(1) gauge bosons and string physics at the forward physics facility. *Phys. Lett. B*, 832:137253, 2022.
- [26] Pascal Anastasopoulos, Elias Niederwieser, and François Rondeau. Light stringy states and the $g - 2$ of the muon. *JHEP*, 11:120, 2022.
- [27] Pascal Anastasopoulos, Kunio Kaneta, Elias Kiritsis, and Yann Mambrini. Anomalous and axial Z' contributions to $g-2$. *JHEP*, 02:051, 2023.
- [28] J. Wess and B. Zumino. Consequences of anomalous Ward identities. *Phys. Lett. B*, 37:95–97, 1971.
- [29] Roberta Armillis, Claudio Coriano, and Marco Guzzi. Trilinear Anomalous Gauge Interactions from Intersecting Branes and the Neutral Currents Sector. *JHEP*, 05:015, 2008.
- [30] Pascal Anastasopoulos, Francesco Fucito, Andrea Lionetto, Gianfranco Pradisi, Antonio Racioppi, and Yassen S. Stanev. Minimal Anomalous U(1)-prime Extension of the MSSM. *Phys. Rev. D*, 78:085014, 2008.
- [31] Michael B. Green and John H. Schwarz. Anomaly Cancellation in Supersymmetric D=10 Gauge Theory and Superstring Theory. *Phys. Lett. B*, 149:117–122, 1984.
- [32] Michael B. Green, Jeffrey A. Harvey, and Gregory W. Moore. I-brane inflow and anomalous couplings on d-branes. *Class. Quant. Grav.*, 14:47–52, 1997.
- [33] Pascal Anastasopoulos, M. Bianchi, E. Dudas, and E. Kiritsis. Anomalies, anomalous U(1)’s and generalized Chern-Simons terms. *JHEP*, 11:057, 2006.
- [34] Claudio Coriano, Marco Guzzi, and Simone Morelli. Unitarity Bounds for Gauged Axionic Interactions and the Green-Schwarz Mechanism. *Eur. Phys. J. C*, 55:629–652, 2008.
- [35] Roberta Armillis, Claudio Coriano, Marco Guzzi, and Simone Morelli. Axions and Anomaly-Mediated Interactions: The Green-Schwarz and Wess-Zumino Vertices at Higher Orders and $g-2$ of the muon. *JHEP*, 10:034, 2008.
- [36] Claudio Coriano, Nikos Irges, and Simone Morelli. Stuckelberg axions and the effective action of anomalous Abelian models. 1. A Unitarity analysis of the Higgs-axion mixing. *JHEP*, 07:008, 2007.
- [37] W. B. Atwood et al. The Large Area Telescope on the Fermi Gamma-ray Space Telescope Mission. *Astrophys. J.*, 697:1071–1102, 2009.
- [38] M. Ackermann et al. Updated search for spectral lines from Galactic dark matter interactions with pass 8 data from the Fermi Large Area Telescope. *Phys. Rev. D*, 91(12):122002, 2015.
- [39] M. Actis et al. Design concepts for the Cherenkov Telescope Array CTA: An advanced facility for ground-based high-energy gamma-ray astronomy. *Exper. Astron.*, 32:193–316, 2011.
- [40] S. Abe et al. Dark Matter Line Searches with the Cherenkov Telescope Array. 3 2024.
- [41] H. Abdallah et al. Search for γ -Ray Line Signals from Dark Matter Annihilations in the Inner Galactic Halo from 10 Years of Observations with H.E.S.S. *Phys. Rev. Lett.*, 120(20):201101, 2018.
- [42] Mariangela Lisanti. Lectures on Dark Matter Physics. In *Theoretical Advanced Study Institute in Elementary Particle Physics: New Frontiers in Fields and Strings*, pages 399–446, 2017.

- [43] Paolo Gondolo and Graciela Gelmini. Cosmic abundances of stable particles: Improved analysis. *Nucl. Phys. B*, 360:145–179, 1991.
- [44] N. Aghanim et al. Planck 2018 results. VI. Cosmological parameters. *Astron. Astrophys.*, 641:A6, 2020. [Erratum: *Astron. Astrophys.* 652, C4 (2021)].
- [45] Alexander Pukhov. An introduction to micrOMEGAs. *PoS, CompTools2021*:037, 2022.
- [46] Mark Srednicki, Richard Watkins, and Keith A. Olive. Calculations of Relic Densities in the Early Universe. *Nucl. Phys. B*, 310:693, 1988.
- [47] Julio F. Navarro, Carlos S. Frenk, and Simon D. M. White. A Universal density profile from hierarchical clustering. *Astrophys. J.*, 490:493–508, 1997.